



Adjoint Sensitivity to Potential Vorticity during the Rapid Intensification of Typhoon Surigae (2021)

#78

Nuo Chen and Michael Morgan

Department of Atmospheric and Oceanic Sciences, University of Wisconsin-Madison

Background and Motivation

Rather than interpreting the adjoint sensitivity of a forecast response to individual state variables, consideration of the sensitivity to the potential vorticity may provide clearer dynamical insights, similar to the “PV thinking”. Here, we calculate the sensitivities to quasi-geostrophic potential vorticity (QGPV, \hat{q}), to an imbalance (\hat{a}) to the geostrophically balanced states ($\hat{u}_g, \hat{v}_g, \hat{\theta}_g$), and to the ageostrophic wind ($\hat{u}_{ag}, \hat{v}_{ag}$) from the adjoint output of the Weather Researching and Forecasting (WRF) model version 3.8.1.

The goals of this presentation include:

1. showing that initializing the adjoint model with a balanced forcing reduces the amplitude of the high frequency wave patterns associated to adjoint adjustment;
2. diagnosing and describing the sensitivities to balanced and imbalanced fields for the case of Super Typhoon Surigae.

Case Study: Super Typhoon Surigae (2021)

Rapid intensification (55 kt to 80 kt) in 24 hours beginning 0600 UTC 15 April

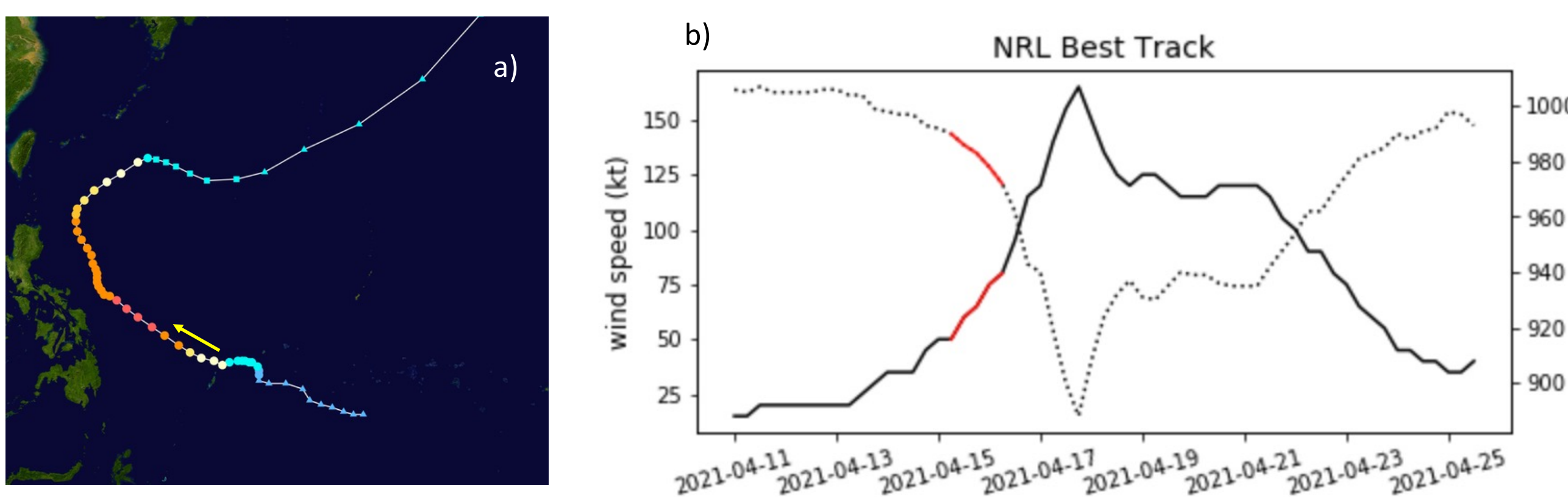


Figure 1: NRL Best Track (a) path (b) intensity

Synoptics of Surigae

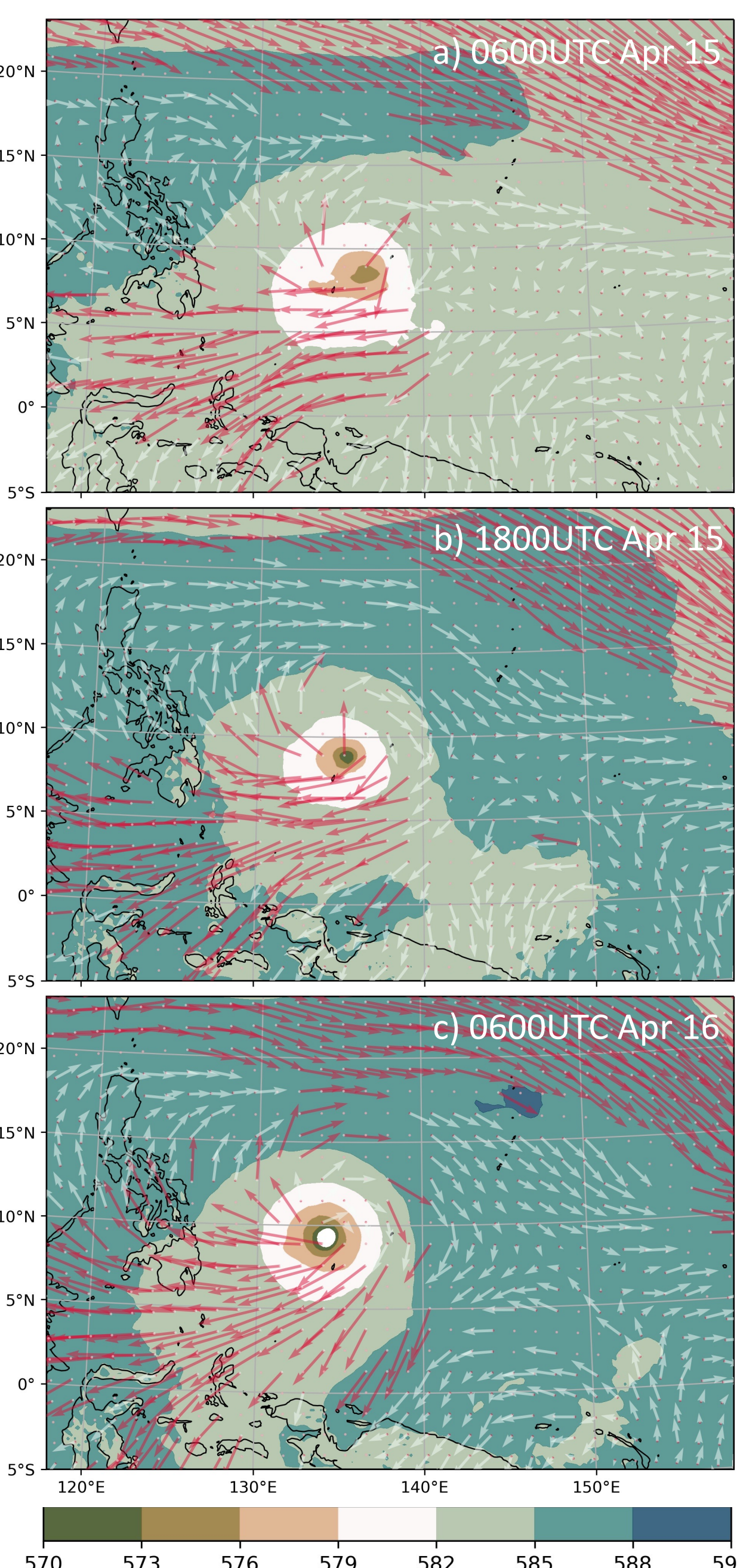


Figure 2: Synoptic evolution as the Surigae intensifies. 500 hPa geopotential height is shaded (3 dam) and 850-200 hPa wind shear vectors (white: $\leq 15 \text{ ms}^{-1}$, red: $\geq 20 \text{ ms}^{-1}$). Persistent strong wind shear south to the storm throughout the simulation time.

Model Setup

WRF/WRFPLUS V3.8.1

- 0.25° GFS FNL
- 24 km grid spacing and 41 vertical levels to 50 hPa
- $R = -\bar{\mu}$ (column dry air mass) within the 995 hPa contour at 0600 UTC 16 April

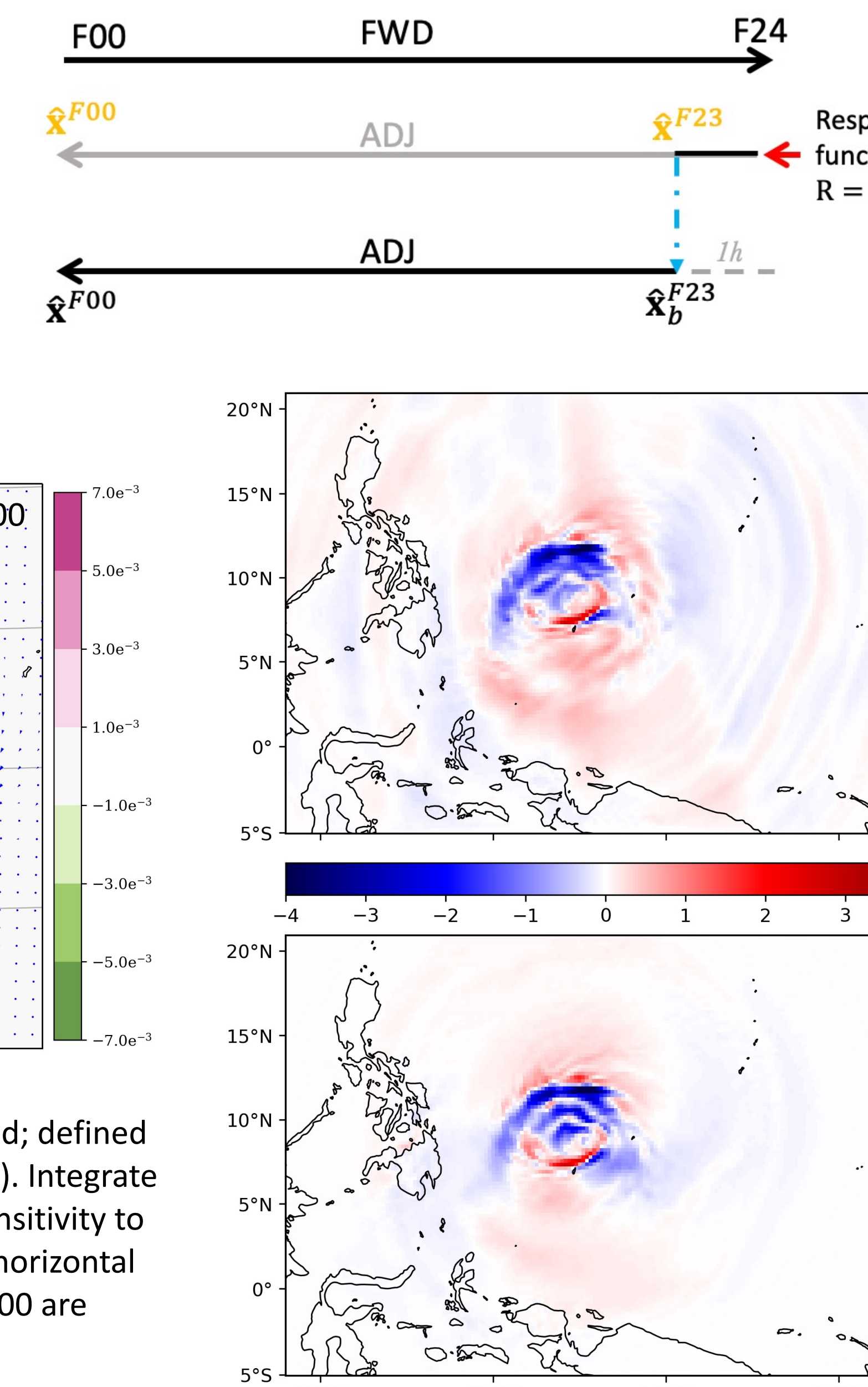


Figure 3: Response function area (meshed; defined from F24 wrf output where $\text{slp} \leq 995 \text{ hPa}$). Integrate backwards from F24 to F00. Here, the sensitivity to dry column air $\hat{\mu}$ (shaded), sensitivity to horizontal winds at 900 hPa (arrows; Pa sm^{-1}) at F00 are plotted.

Figure 4: Response sensitivity to the zonal wind at 900 hPa at F14 (10 h backward integration) from a) simply set $R = -\bar{\mu}$ b) with sensitivity to geostrophically balanced states as the adjoint forcing.

- The balanced adjoint forcing/response function is able to filter out the gravity wave pattern due to adjustment process among different adjoint fields.

Diagnostic Tools

For simplicity, denote $\frac{\partial R}{\partial x} = \hat{x}$

Following Arbogast (1998), QGPV and geostrophic balance are:

$$\begin{cases} q' = \nabla^2 \psi' + \frac{\partial}{\partial p} \left(\frac{f_0}{S} \frac{\partial}{\partial p} \right) \phi' \\ a = \psi' - \frac{1}{f_0} \phi' \end{cases}$$

derive sensitivity to QGPV and to imbalance as

$$\begin{cases} \left[\nabla^2 + \frac{\partial}{\partial p} \left(\frac{f_0}{S} \frac{\partial}{\partial p} \right) \right] \hat{q} = \frac{1}{f_0} \hat{\psi} + \hat{\phi} \\ \left[\nabla^2 + \frac{\partial}{\partial p} \left(\frac{f_0}{S} \frac{\partial}{\partial p} \right) \right] \hat{a} = \frac{\partial}{\partial p} \left(\frac{f_0}{S} \frac{\partial}{\partial p} \right) \hat{\psi} - \nabla^2 \hat{\phi} \end{cases}$$

Further, derive the sensitivity to the geostrophically balanced states

$$\begin{cases} \hat{u}_g = \frac{\partial \hat{q}}{\partial y} & \hat{x} = (\hat{u}, \hat{v}, \hat{\theta}) \\ \hat{v}_g = -\frac{\partial \hat{q}}{\partial x} & \hat{q} \\ \hat{\theta}_g = \frac{f_0 \gamma \partial \hat{q}}{S \partial p} & \hat{x}_b = (\hat{u}_g, \hat{v}_g, \hat{\theta}_g, \hat{\phi}_g) \end{cases}$$

And the sensitivity to the ageostrophic winds

$$\begin{cases} \nabla^2 \hat{u}_{ag} = \frac{\partial}{\partial y} (\hat{\psi} - \nabla^2 \hat{q}) - \frac{\partial \hat{\lambda}}{\partial x} \\ \nabla^2 \hat{v}_{ag} = -\left(\frac{\partial}{\partial x} (\hat{\psi} - \nabla^2 \hat{q}) + \frac{\partial \hat{\lambda}}{\partial y} \right) \end{cases}$$

Vertical Cross Section of QG Balanced Sensitivity Fields

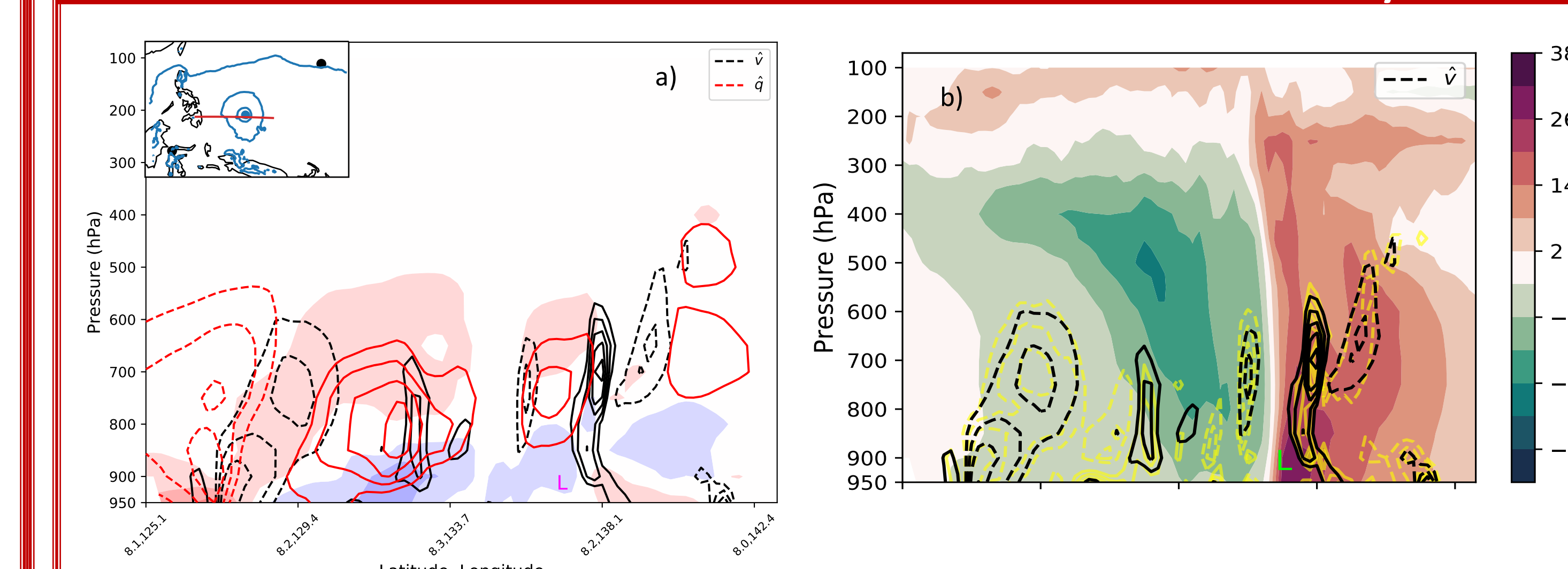


Figure 5: QG balanced sensitivity cross sections at F00 a) sensitivities to geostrophic meridional winds \hat{v}_g (black contours; 0.4 Pa sm^{-1} interval), to balanced potential temperature $\hat{\theta}$ (shaded, Pa K^{-1}) and to QGPV \hat{q} (red contour; Pa s) b) \hat{v}_g (black contours), full sensitivity to meridional wind \hat{v} (yellow contour), and the background meridional wind speed v from wrfout (shaded; ms^{-1})

- A positive sensitivity to QGPV \hat{q} is surrounded by cyclonic vector sensitivity to winds \hat{u} , with a positive sensitivity to potential temperature $\hat{\theta}$ above and a negative $\hat{\theta}$ below (Fig. 5a);

- Fig. 5b shows the geostrophically balanced \hat{v}_g can catch most of full sensitivity \hat{v} 's characteristics, but missing a few boundary layer and inner core features. This is addressed by the ageostrophic component of the sensitivity to winds.

Reference

- Arbogast, P., 1998: Sensitivity to potential vorticity. *Quart. J. Roy. Meteor. Soc.*, **124**, 1605-1615.
 Kleist, D. T., and M. C. Morgan, 2005a: Interpretation of the structure and evolution of adjoint-derived forecast sensitivity gradients. *Mon. Wea. Rev.*, **133**, 466-484.
 Orr, W. M., 1907: Stability or instability of the steady motions of a perfect liquid. *Proc. Roy. Irish Acad.*, **27**, 9-69.
 Nolan, D. S., and B. F. Farrell (1999), Generalized stability analyses of asymmetric disturbances in one- and two-celled vortices maintained by radial inflow, *J. Atmos. Sci.*, **56**, 1282-1307.

QG and Imbalance Sensitivities Analysis

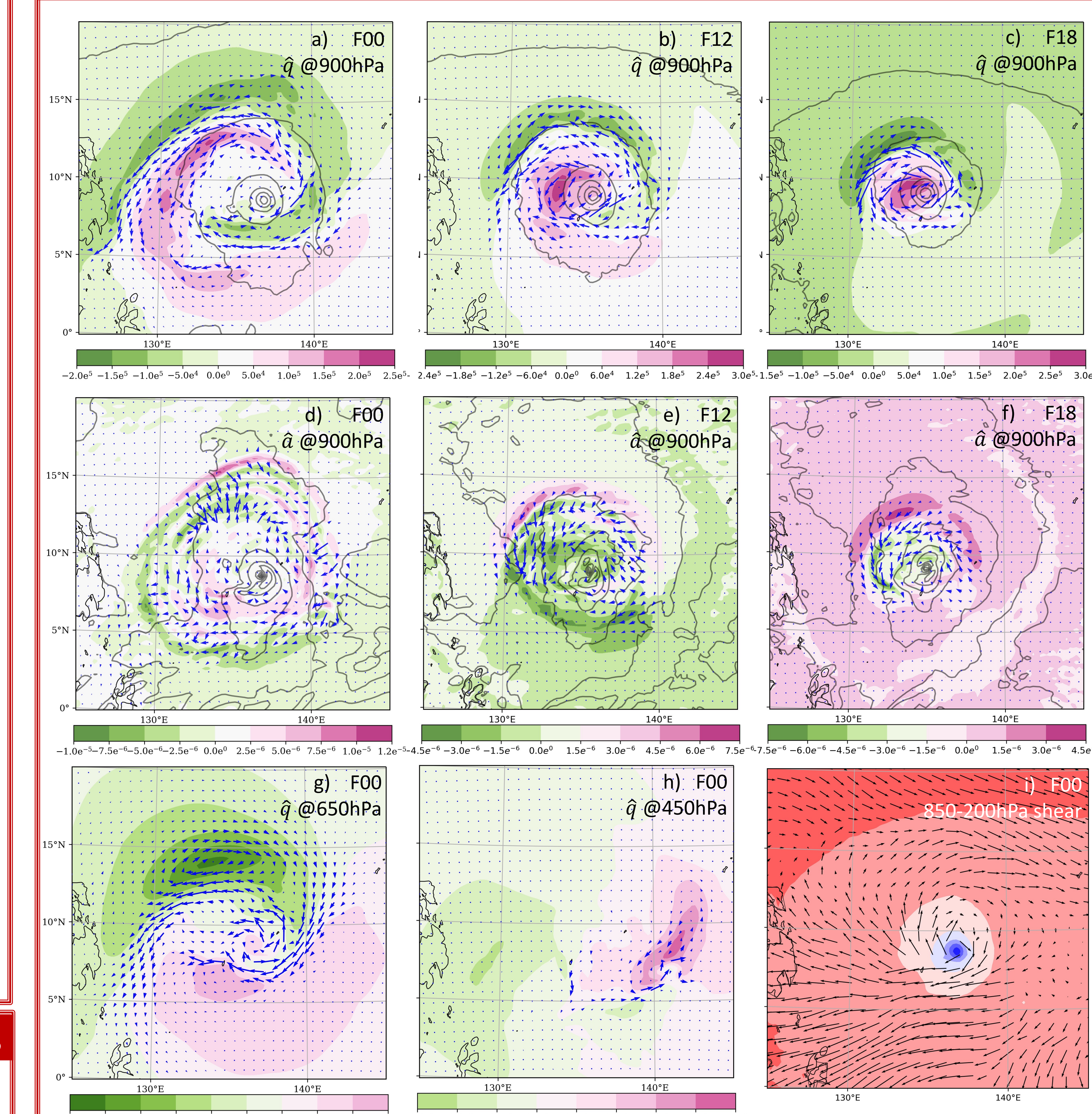


Figure 6: The sensitivity to QGPV (\hat{q} ; shaded) and sensitivity to geostrophically balanced winds \hat{v}_g (arrow) at 950 hPa at a) F00, b) F12, c) F18 with slp (contour), and at F00 for g) 650 hPa and h) 450hPa. Sensitivity to the imbalance (\hat{a} ; shaded; Pa s m^{-2}) and sensitivity to the ageostrophic winds \hat{v}_{ag} (arrow) at 950 hPa at d) F00, e) F12, and f) F18 with 10 m wind speed (contour). i) 850-200 hPa layer wind shear vector at F00 and slp.

- In Fig. 6a, such sensitivity field (not cyclonic around the TC center at F00) is difficult to interpret without the help of \hat{q} ;
- positive \hat{q} starts from the NW of the storm and get advected into the center of the storm with time. \hat{q} is able to explain the rotating part of the sensitivity to winds, while the sensitivity to the ageostrophic wind in the boundary layer is able to capture the contribution from the inflow to the intensification of Surigae.

- The 850-200 hPa anticyclonic shear (e.g. Fig. 6i) suggest the possibility of untwisting \hat{q} (e.g. Fig. 6a → h → g), leading to a superposition of the positive QGPV right above our response function area at the final time. This is similar to the Orr mechanism (Orr 1907) discussed in Nolan and Farrell (1999).

Summary and Future Work

1. Use of a balanced adjoint forcing eliminates some of the high frequency wave patterns in the adjoint sensitivity output;
2. The configuration of balanced sensitivity $\hat{u}_g, \hat{v}_g, \hat{\theta}$ around a positive sensitivity to QGPV \hat{q} is much alike wind and temperature configuration around a positive QGPV. The sensitivity to QGPV is surrounded with cyclonic sensitivity to winds, positive sensitivity to temperature above, and negative sensitivity to temperature below;
3. The sensitivity to the ageostrophic winds captures the requirement for the inflow for a stronger TC in the boundary layer.
4. The sensitivity to the imbalance (\hat{a}) is speculated to be associated with sensitivity to divergence. This needs future investigation.
5. Sensitivity to Ertel PV and imbalances with respect to nonlinear balance is under development.

Acknowledgements

This study was supported by the Space Science Engineering Center/Cooperative Institute for Meteorological Satellite Studies.